Available online at www.sciencedirect.com

ScienceDirect

Ceramics International 40 (2014) 1335–1339

CERAMICS INTERNATIONAL

www.elsevier.com/locate/ceramint

Structure, ferroelectric, piezoelectric and ferromagnetic properties of $BiFeO_3$–$Ba_{0.85}Ca_{0.15}Ti_{0.90}Zr_{0.10}O_3$ lead-free multiferroic ceramics

Dunmin Lin, K.W. Kwok*, H.L.W. Chan

Department of Applied Physics and Materials Research Centre, The Hong Kong Polytechnic University, Kowloon, Hong Kong, China

Received 8 April 2013; received in revised form 2 July 2013; accepted 2 July 2013
Available online 8 July 2013

Abstract

Lead-free $(1-x)BiFeO_3$–$xBa_{0.85}Ca_{0.15}Ti_{0.90}Zr_{0.10}O_3$+1 mol% MnO_2 multiferroic ceramics have been prepared by a conventional ceramic fabrication technique and their structure, ferroelectric, piezoelectric and ferromagnetic properties have been studied. $Ba_{0.85}Ca_{0.15}(Ti_{0.9}Zr_{0.1})O_3$ diffuses into the $BiFeO_3$ lattices to form a new solid solution with a perovskite structure. The ceramics with $x=0.15$–0.275 possess a rhombohedral phase. As x increases, the ceramic transforms into a pseudo-cubic phase. A morphotropic phase boundary separating the two phases is formed at $0.275 < x < 0.30$. A diffusive ferroelectric–paraelectric phase transition is induced in the ceramics with high concentrations of $Ba_{0.85}Ca_{0.15}(Ti_{0.9}Zr_{0.1})O_3$. The ferroelectric and piezoelectric properties of the ceramics are improved. For the ceramic with $x=0.275$, the piezoelectric properties become optimum: $d_{33}=106$ pC/N and $k_p=29.7\%$. The ceramics also exhibit weak magnetic properties.

Keywords: Lead-free; Multiferroic; Ferroelectric; Ferromagnetic

1. Introduction

Perovskite lead-based ceramics such as $Pb(Ti,Zr)O_3$, $Pb(Mg_{1/3}Nb_{2/3})O_3$–$PbTiO_3$ have been widely used in actuators and sensors because of their excellent piezoelectric properties near the morphotropic phase boundary (MPB). However, the use of these ceramics has led to serious environmental problems because of the strong toxicity of lead oxide. Therefore, it is necessary to develop lead-free ferroelectric and piezoelectric ceramics.

$BiFeO_3$ is a rhombohedral ferroelectric with perovskite structure and possesses a very high Curie temperature ($T_C=830$ °C) [1,2]. In recent years, being one of the few single-phase multiferroics, $BiFeO_3$-based perovskite materials have attracted considerable attention and their ferroelectric and ferromagnetic properties have been studied extensively [3–6]. $BiFeO_3$ ceramic generally exhibits high electrical leakage, which is resulted from the reduction of Fe^{3+} to Fe^{2+} during sintering and the formation of oxygen vacancies for charge compensation [7,8]. This semiconducting nature of $BiFeO_3$ leads to difficulties in obtaining saturated polarization hysteresis loop and electrical poling for evaluating the piezoelectric properties of the ceramic. To improve the electrical insulation, ABO_3-type perovskite compounds such as $CaTiO_3$ [9], $SrTiO_3$ [10], $BaTiO_3$ [8], and $Bi_{0.5}K_{0.5}TiO_3$ [11] have been used to form new solid solutions with $BiFeO_3$. These studies mainly focus on the multiferroic properties of the materials. Recently, a lead-free solid solution $Ba_{0.85}Ca_{0.15}Ti_{0.90}Zr_{0.10}O_3$ with excellent piezoelectricity ($d_{33}\sim620$ pC/N) [12], strong ferroelectricity ($P_r\sim13$ μC/cm^2 and $E_c\sim0.27$ kV/mm) [13] but a low Curie temperature (~93 °C) has been developed. In the present work, a new lead-free solid solution of $(1-x)BiFeO_3$–$xBa_{0.85}Ca_{0.15}Ti_{0.90}Zr_{0.10}O_3$ added with a MnO_2 sintering aid was prepared by a conventional mixed oxide method, and its phase transition, ferroelectric, piezoelectric and ferromagnetic properties were studied. MnO_2 sintering aid is effective in improving the electrical insulation of perovskite ceramics [14].

*Corresponding author. Tel.: +852 27665667; fax: +852 23337629.
E-mail address: apkwkwok@polyu.edu.hk (K.W. Kwok).

0272-8842/$ - see front matter © 2013 Elsevier Ltd and Techna Group S.r.l. All rights reserved.
http://dx.doi.org/10.1016/j.ceramint.2013.07.014

2. Experimental

$(1-x)BiFeO_3$–$xBa_{0.85}Ca_{0.15}Ti_{0.90}Zr_{0.10}O_3$+1 mol%$MnO_2$ (BFO–BCTZ–x) ceramics were prepared by a conventional mixed oxide method using analytical-grade metal oxides and carbonate powders: $BaCO_3$ (99%), $CaCO_3$ (99%), ZrO_2 (99%), Bi_2O_3 (99.9%), Fe_2O_3 (99.9%), TiO_2 (99.9%) and MnO_2 (99%). The powders in the stoichiometric ratio of $(1-x)BiFeO_3$–$xBa_{0.85}Ca_{0.15}Ti_{0.90}Zr_{0.10}O_3$ were first mixed thoroughly in ethanol using zirconia balls for 10 h. After the calcination at 800 °C for 4 h, MnO_2 powder was added. The mixture was ball-milled again for 8 h and mixed thoroughly with a poly(vinyl alcohol) binder solution, and then pressed into disk samples. After removal of the binder, the samples were sintered at 960 °C for 2 h. Silver electrodes were fired on the top and bottom surfaces of the sintered ceramics at 810 °C for 10 min. The ceramics were poled under a dc field of 5 kV/mm at 90 °C in a silicone oil bath for 40 min.

X-ray diffraction (XRD) analysis with CuK_β radiation (SmartLab, Rigaku Co., Japan) was used to identify the crystalline structure of the ceramics. The surface microstructures were observed using scanning electron microscopy (JSM-5900LV, JEOL, Japan). An LCR meter (Agilent E4980A, USA) was used to measure the temperature dependence of the relative permittivity ε_r of the ceramics. The polarization hysteresis (P–E) loop was measured at room temperature using a standard ferroelectric test unit (Premier II, Radiant Technologies). The planar electromechanical coupling factor, k_p, was determined by the resonance method according to the IEEE Standards 176 using an impedance analyzer (Agilent 4294 A, USA). The piezoelectric constant, d_{33}, was measured using a piezo-d_{33} meter (ZJ-3d, Beijing, China). The magnetic hysteresis (M–H) loop was measured using a vibrating sample magnetometer (VSM, Lakeshore 7300, USA).

3. Results and discussion

Fig. 1 shows the XRD patterns of the BFO–BCTZ–x ceramics. All the ceramics exhibit a pure perovskite structure and no secondary phase is observed (Fig. 1a). These indicate that $Ba_{0.85}Ca_{0.15}(Ti_{0.9}Zr_{0.1})O_3$ have diffused into the $BiFeO_3$ lattices to form a new solid solution. The concentration of $Ba_{0.85}Ca_{0.15}(Ti_{0.9}Zr_{0.1})O_3$ (i.e., x) has an important influence on the crystalline structure of the ceramics (Fig. 1b). The ceramic with $x=0.15$ possess a rhombohedral structure, which can be evidenced by the splitting of the two diffraction peaks near 57.5°. As x increases, the split diffraction peaks gradually merge into a single peak, indicating that the ceramic has transformed into a pseudocubic phase. These results suggest that a MPB between the rhombohedral and pseudocubic phases is formed in the BFO–BCTZ–x ceramics with $0.275 \leq x \leq 0.30$.

Fig. 2 shows the SEM micrographs of the BFO–BCTZ–x ceramics with $x=0.15$ and 0.25 sintered at 960 °C for 2 h. Although the sintering temperature is low (960 °C), the ceramics are dense and pore-free, having a high relative density ($>95\%$) measured by the Archimedes method. For the ceramic with $x=0.15$, the grains have an average size of about 3 μm (Fig. 2a). As x increases to 0.25, the grains become significantly larger and exhibit a bimodal distribution, with large grains of size 10–15 μm uniformly distributed among small grains of size 5–6 μm (Fig. 2b). The abnormal grain

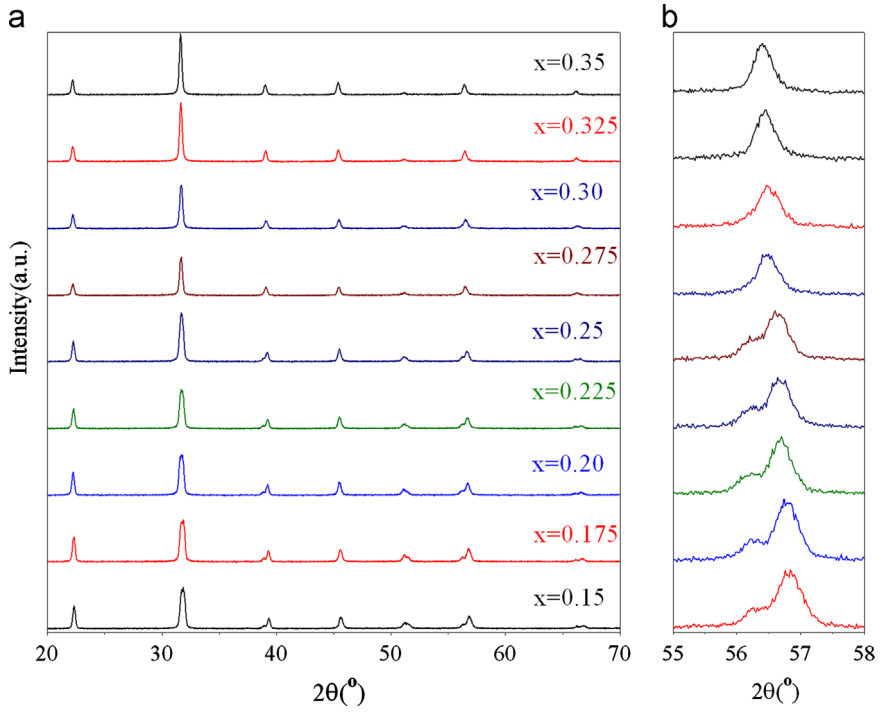

Fig. 1. XRD patterns of the BFO–BCTZ–x ceramics.

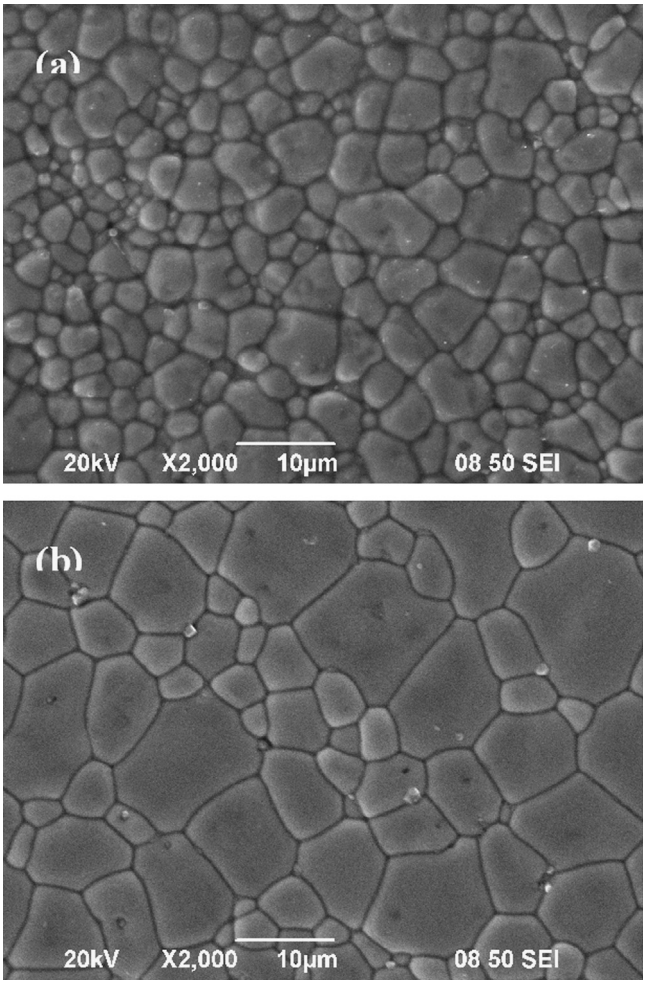

Fig. 2. SEM micrographs of the BFO–BCTZ–x ceramics sintered at 960 °C for 2 h: (a) $x=0.15$ and (b) $x=0.25$.

growth may be resulted from a much larger growth rate of some large grains as compared with small matrix grains according to two-dimensional nucleation theories [15].

The temperature dependences of ε_r at 1 kHz for the BFO–BCTZ–x ceramics are shown in Fig. 3a–c, while the variation of Curie temperature, T_C, with x is shown in Fig. 3d. It is known that $BiFeO_3$ has a high T_C of 830 °C. As shown in Fig. 3a, no dielectric peak is observed in the temperature range studied, from 20 °C to 700 °C, for the ceramics with $x=0.15$ and 0.175, suggesting that their T_C should be above 700 °C. On the other hand, the dielectric peak associated with the ferroelectric to paraelectric phase transition is observed for the ceramics with $x=0.20$–0.35 (Fig. 3b–c). As shown in Fig. 3d, the observed T_C decreases from 690 °C to 390 °C as x increases from 0.20 to 0.30, and then increases to 490 °C at $x=0.35$. It can also be seen that the ceramic with $x=0.20$ exhibits a sharp phase transition peak at T_C (Fig. 3b), suggesting that it is a normal ferroelectric. As x increases, the transition peak becomes broadened gradually, suggesting that a diffusive ferroelectric–paraelectric phase transition is induced. This should be ascribed to the increase in the degree of cation disorder and the local compositional fluctuation caused by the partial substitutions of Ba^{2+}/Ca^{2+} for Bi^{3+} and Ti^{4+}/Zr^{4+} for Fe^{3+} in the $BiFeO_3$ lattices.

Fig. 4a shows the P–E loops of the BFO–BCTZ–x ceramics, while the variations of the remanent polarization, P_r, and coercive field, E_c, with x are shown in Fig. 4b. All the ceramics can withstand a high electric field of 8–10 kV/mm without electric breakdown, implying that they possess good electrical insulation and can be poled effectively. A typical P–E loop cannot be obtained for the BFO–BCTZ–0.15 ceramic. Even under an electric field of 10 kV/mm, the ceramic exhibits an almost linear relationship between electric field and polarization, giving a "line" with a nearly zero value of P_r (0.34 μC/cm^2) as shown in Fig. 4a. As x increases, a typical P–E loop can be obtained, and the observed P_r and E_c increase with increasing x (Fig. 4b). For the ceramics with $x=0.25$–0.30, a well-saturated and square-like P–E loop is obtained (Fig. 4a), giving a large P_r (20.3–24.5 μC/cm^2) and a high E_c (4.91–5.93 kV/mm). However, as x further increases, the ferroelectricity of the ceramics becomes degraded (Fig. 4b). As shown in Fig. 4a, the BFO–BCTZ–0.35 ceramic exhibits a very slim and slanted P–E loop with a small P_r (11.9 μC/cm^2) and a low E_c (3.04 kV/mm) (Fig. 4a), which should be ascribed to the existence of nonpolar phase in the ceramic.

Fig. 5 shows the composition dependences of piezoelectric and dielectric properties of the BFO–BCTZ–x ceramics. Although all the ceramics can withstand a high electric field of 8–10 kV/mm without electric breakdown, it is not easy to pole them effectively at room temperature because of their high coercive field (up to 6 kV/mm, Fig. 4b). The ceramics were then poled at elevated temperatures (90 °C) in the present study for inducing their piezoelectric properties. As shown in Fig. 5a, the observed d_{33} increases from 4 pC/N to 106 pC/N as x increases from 0.15 to 0.275, and then decrease abruptly to 2 pC/N with further increasing x to 0.35. The observed k_p exhibits a similar compositional dependence and gives a maximum value of 29.7% at $x=0.275$. The observed ε_r increases from 180 to 512 with increasing x from 0.15 to 0.275, and then remains almost unchanged. On the other hand, the observed $\tan\delta$ decreases from 7.49% to 1.61% as x increases from 0.15 to 0.225, and then increases to 4.01% at $x=0.35$. The improvement in the piezoelectricity of the ceramics should be attributed to the enhanced ferroelectricity and electrical insulation.

Fig. 6 shows the M–H loops of the BFO–BCTZ–x ceramics with $x=0.15$, 0.225, 0.275 and 0.35 measured under a low magnetic field of 10 kOe. All the ceramics exhibit a typical M–H loops, exemplifying the ferromagnetic ordering and weak magnetization in the ceramics. The observed remanent magnetization M_r for the ceramics with $x=0.15$ and 0.225 are similar ($\sim$0.0055 emu/g). However, the observed M_r decreases with further increasing x. It has been known that $BiFeO_3$ is an anti-ferromagnetic with a magnetic structure of G-type. However, there exists a spiral spin structure with an incommensurate spiral period of $\sim$62 nm superimposed on the anti-ferromagnetic ordering, leading to a cancellation of macroscopic magnetization.[10] Probably due to the partial substitutions of Ba^{2+}/Ca^{2+} for Bi^{3+} and Ti^{4+}/Zr^{4+} for Fe^{3+},

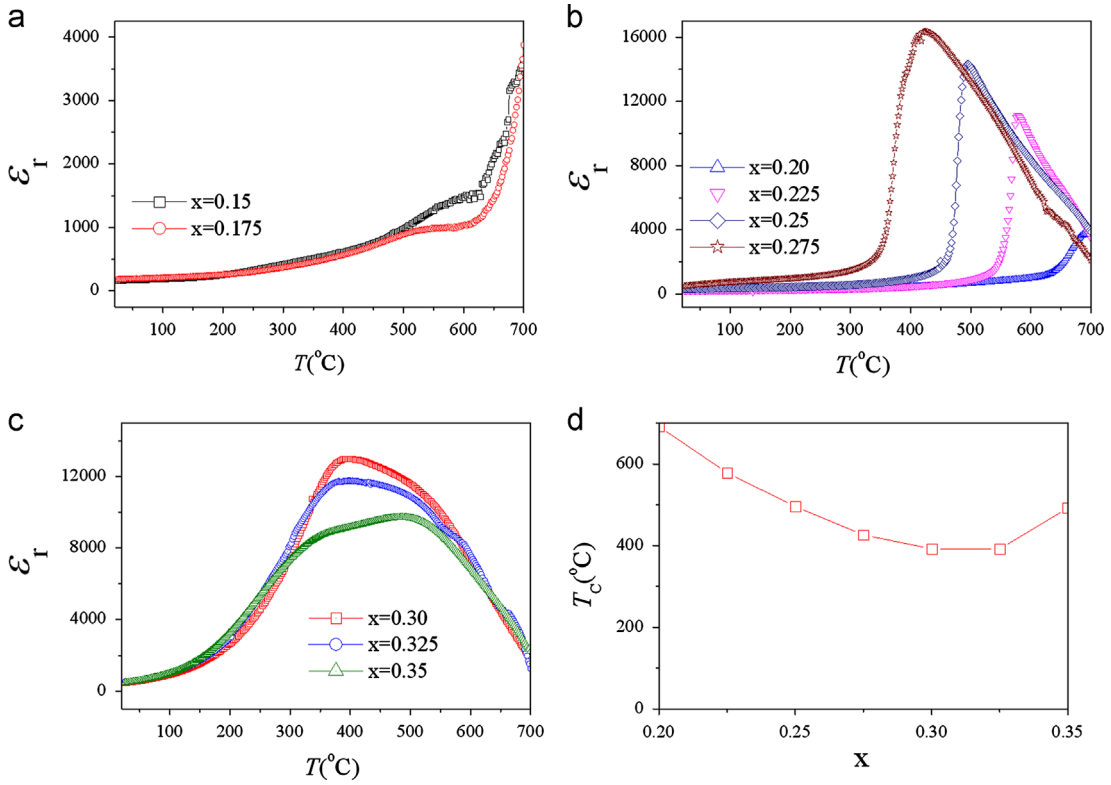

Fig. 3. (a–c) Temperature dependence of ε_r at 1 kHz for the BFO–BCTZ–x ceramics and (d) variation of T_C with x for the BFO–BCTZ–x ceramics.

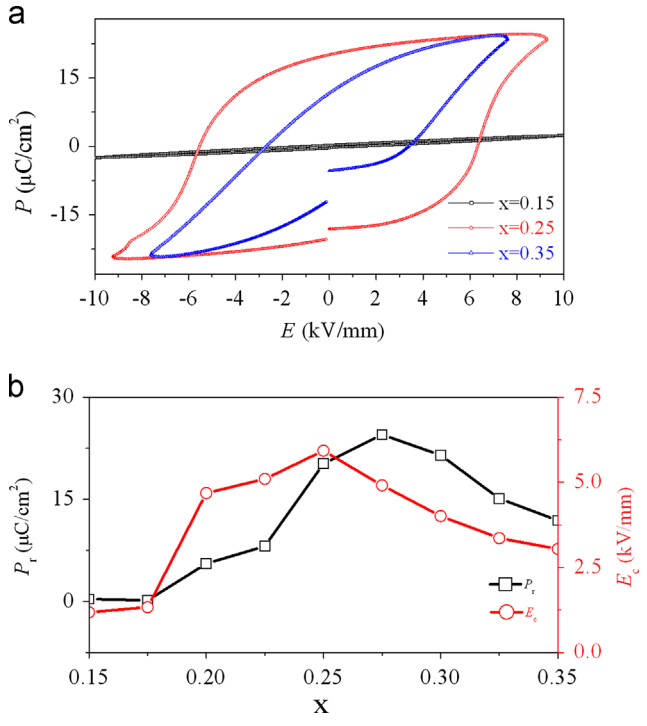

Fig. 4. (a) P–E loops for the the BFO–BCTZ–x ceramics; (b) variations of P_r and E_c of with x for the BFO–BCTZ–x ceramics.

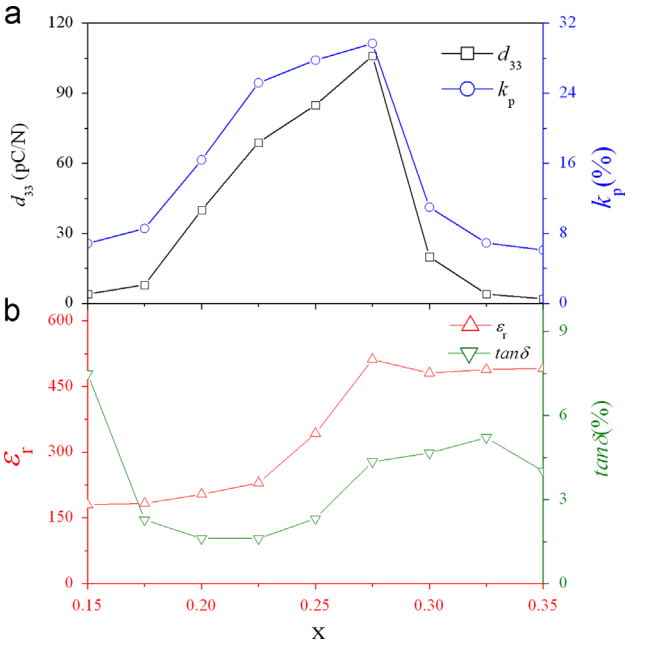

Fig. 5. Variations of d_{33}, k_p, ε_r and tan δ with x for the BFO–BCTZ–x ceramics.

the spatially modulated spin order in the BFO–BCTZ–x ceramics are suppressed, and thus releasing the locked magnetization and enhancing the magnetic properties.[10,16]

4. Conclusion

New lead-free (1–x)$BiFeO_3$–$xBa_{0.85}Ca_{0.15}Ti_{0.90}Zr_{0.10}O_3$+1 mol % MnO_2 multiferroic ceramics have been prepared by a conventional ceramic fabrication technique and their phase transition,

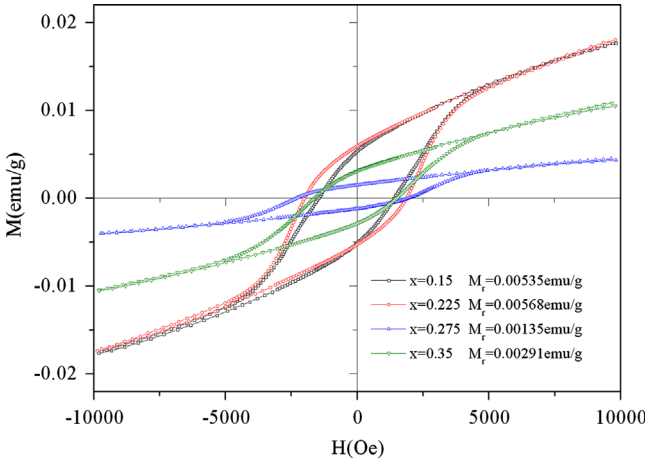

Fig. 6. M–H loops for the BFO–BCTZ–x ceramics with $x=0.15$, 0.225, 0.275 and 0.35.

ferroelectric and piezoelectric properties have been studied. Our results show that $Ba_{0.85}Ca_{0.15}(Ti_{0.9}Zr_{0.1})O_3$ diffuses into the $BiFeO_3$ lattices to form a new solid solution with a perovskite structure. As the concentration of $Ba_{0.85}Ca_{0.15}(Ti_{0.9}Zr_{0.1})O_3$ increases, the crystal structure of the ceramics transforms from rhombohedral to pseudo-cubic. A morphotropic phase boundary separating the two phases is formed at $0.275 < x < 0.30$. Strong ferroelectricity ($P_r \sim 20.3$–24.5 μC/cm^2) is observed in the ceramics with $x=0.25$–0.30. The ceramic with $x=0.275$ exhibits the optimum piezoelectric properties: $d_{33}=106$ pC/N and $k_p=29.7\%$. The ceramics also exhibit weak magnetic properties.

Acknowledgments

This work was supported by the Research Committee (A/C code 1-ZV9B) and the Centre for Smart Materials of The Hong Kong Polytechnic University.

References

[1] Y.P. Wang, L. Zhou, M.F. Zhang, X.Y. Chen, J.M. Liu, Z.G. Liu, Room-temperature saturated ferroelectric polarization in $BiFeO_3$ ceramics synthesized by rapid liquid phase sintering, Applied Physics Letters 84 (2004) 1731–1733.

[2] M. Kumar, K.L. Yadav, Magnetic field induced phase transition in multiferroic $BiFe_{1-x}Ti_xO_3$ ceramics prepared by rapid liquid phase sintering, Applied Physics Letters 91 (2007) 112911.

[3] T. Kawae, Y. Terauchi, H. Tsuda, M. Kumeda, A. Morimoto, Improved leakage and ferroelectric properties of Mn and Ti codoped $BiFeO_3$ thin films, Applied Physics Letters 94 (2009) 112904.

[4] M.S. Wu, Z.B. Huang, C.X. Han, S.L. Yuan, C.L. Lu, S.C. Xia, Enhanced multiferroic properties of $BiFeO_3$ ceramics by Ba and high-valence Nb co-doping, Solid State Communications 152 (2012) 2142–2146.

[5] Q. Zhang, X. Zhu, Y. Xu, H. Gao, Y. Xiao, D. Liang, J. Zhu, J. Zhu, D. Xiao, Effect of La^{3+} substitution on the phase transitions, micro-structure and electrical properties of $Bi_{1-x}La_xFeO_3$ ceramics, Journal of Alloys and Compounds 546 (2012) 57–62.

[6] K.S. Nalwa, A. Garg, Phase evolution, magnetic and electrical properties in Sm-doped bismuth ferrite, Journal of Applied Physics 103 (2008) 044101.

[7] M.M. Kumar, A. Srinivas, S.V. Suryanarayana, Structure property relations in $BiFeO_3$/$BaTiO_3$ solid solutions, Journal of Applied Physics 87 (2000) 855–862.

[8] T.H. Wang, Y. Ding, C.S. Tu, Y.D. Yao, K.T. Wu, T.C. Lin, H.H. Yu, C.S. Ku, H.Y. Lee, Structure, magnetic, and dielectric properties of $(1-x)BiFeO_3$–$xBaTiO_3$ ceramics, Journal of Applied Physics 109 (2011) 07D907.

[9] Q.Q. Wang, Z. Wang, X.Q. Liu, X.M. Chen, Improved structure stability and multiferroic characteristics in $CaTiO_3$-modified $BiFeO_3$ ceramics, Journal of the American Ceramic Society 95 (2012) 670–675.

[10] Z.Z. Ma, Z.M. Tian, J.Q. Li, C.H. Wang, S.X. Huo, H.N. Duan, S. L. Yuan, Enhanced polarization and magnetization in multiferroic $(1-x)$ $BiFeO_3$–$xSrTiO_3$ solid solution, Solid State Sciences 13 (2011) 2196–2200.

[11] H. Matsuo, Y. Noguchi, M. Miyayama, M. Suzuki, A. Watanabe, Structural and piezoelectric properties of high-density $(Bi_{0.5}K_{0.5})TiO_3$–$BiFeO_3$ ceramics, Journal of Applied Physics 108 (2010) 104103.

[12] W. Liu, X. Ren, Large piezoelectric effect in Pb-free ceramics, Physical Review Letters 103 (2009) 257602.

[13] S. Su, R. Zuo, S. Lu, Z. Xu, X. Wang, L. Li, Poling dependence and stability of piezoelectric properties of $Ba(Zr_{0.2}Ti_{0.8})O_3$–$(Ba_{0.7}Ca_{0.3})TiO_3$ ceramics with huge piezoelectric coefficients, Current Applied Physics 11 (2011) S120–S123.

[14] D. Lin, K.W. Kwok, H. Tian, H.W.L. Chan, Phase transitions and electrical properties of $(Na_{1-x}K_x)(Nb_{1-y}Sb_y)O_3$ lead-free piezoelectric ceramics with a MnO_2 sintering aid, Journal of the American Ceramic Society 90 (2007) 1458–1462.

[15] M.S. Kim, D.S. Lee, E.C. Park, S.J. Jeong, J.S. Song, Effect of Na_2O additions on the sinterability and piezoelectric properties of lead-free 95 $(Na_{0.5}K_{0.5})NbO_3$–5$LiTaO_3$ ceramics, Journal of the European Ceramic Society 27 (2007) 4121–4124.

[16] Y. Ma, X.M. Chen, Enhanced multiferroic characteristics in $NaNbO_3$-modified $BiFeO_3$ ceramics, Journal of Applied Physics 105 (2009) 054107.